Journal of Power Sources 625 (2025) 235613

Contents lists available at ScienceDirect

Journal of Power Sources

journal homepage: www.elsevier.com/locate/jpowsour

Functional electrolyte: Design of corrosion inhibition additives to protect Cu current collectors in over-discharged state

Masaki Deguchi [a,c,*], Yanko Marinov Todorov [b], Koji Abe [a,b]

[a] Graduate School of Sciences and Technology for Innovation, Yamaguchi University, 2-16-1 Tokiwadai, Ube, Yamaguchi, 755-8611, Japan
[b] Organization for Research Initiatives, Yamaguchi University, 2-16-1 Tokiwadai, Ube, Yamaguchi, 755-8611, Japan
[c] Panasonic Energy Co., Ltd., 1-1 Matsushita-cho, Moriguchi, Osaka, 570-8511, Japan

HIGHLIGHTS

- *N*,*N*′-dicyclohexylcarbodiimide (DCC) is a new type of Cu corrosion inhibition additive.
- DCC had a high recovery rate of laminated cells after over-discharge.
- Electrolyte with DCC exhibited good discharge capacity and cycling performance.
- DCC complexes were not easily deposited due to their high solubility.
- The analysis suggests that DCC complexes form a thin layer on the Cu surface.

ARTICLE INFO

Keywords:
Electrolyte
Additive
Lithium-ion batteries
Cu current collector

ABSTRACT

Lithium-ion secondary batteries are increasingly being used not only for ICT devices but also for large power sources such as EVs. Typically, the battery module discharge termination voltage is fixed in the device/power supply, but the sequentially connected single cells in the assembled battery may become over-discharged, thus there is a concern that the battery performance is degraded by the dissolution of the Cu current collector. Cu ions diffuse into the electrolyte due to the dissolution of the Cu current collector and precipitate on the anode during charging. This causes blackening of the Cu surface and an increase in cell resistance, and if it progresses further, it may lead to a short circuit. Therefore, we searched for an additive that would improve the battery performance by suppressing the dissolution of Cu, which causes a short circuit during over-discharge. Since 1999, we have proposed a "functional electrolyte" in which a small amount of an additive with a new function is added to the electrolyte. In this work, we focused on additives with carbodiimide groups (-N=C=N-) that prevent dissolution of the Cu collectors during over-discharge and improve the battery performance, and report the finding that *N*,*N*′-dicyclohexylcarbodiimide (DCC) exhibits such a unique behavior.

1. Introduction

We proposed "functional electrolytes" in 1999 and have put many additives into practical use. One example of our prior research that has been reported and put into practical use is that the addition of dinitrile additives, such as adiponitrile (ADN, Fig. 1a) and succinonitrile (SN, Fig. 1b), forms a protective layer on the surface and suppresses corrosion and pitting corrosion of the battery can [1]. We have also found that in the 1 M $LiBF_4$ EC/GBL electrolyte with highly corrosive S=O bonded additives, such as 1,3-propanesultone or ethylene sulfate, the addition of a small amount of ADN or SN forms a protective film on the Al current collector and battery case and corrosion is suppressed [2,3]. More recently, we have found that several triple bond compounds with specific -C≡C- and -C≡N bonds and inorganic phosphates, such as $LiPO_2F_2$, were useful as corrosion inhibiting additives for Al current collectors in the electrolyte of EC/GBL systems using lithium bis (fluorosulfonyl) imide (LiFSI) [4]. Besides our works, much research has been carried out regarding Al corrosion prevention in LiFSI-based electrolytes [5,6]. In this research, we focused on over-discharge, which has not been given much attention, and investigated inhibiting the corrosion of the Cu current collector. The single cells in a sequentially connected assembled battery, such as EVs, may be over-discharged. Metal ions diffuse in the

* Corresponding author. Graduate School of Sciences and Technology for Innovation, Yamaguchi University, 2-16-1 Tokiwadai, Ube, Yamaguchi, 755-8611, Japan.
E-mail address: deguchi.masaki@jp.panasonic.com (M. Deguchi).

https://doi.org/10.1016/j.jpowsour.2024.235613
Received 9 May 2024; Received in revised form 2 October 2024; Accepted 11 October 2024
Available online 29 October 2024

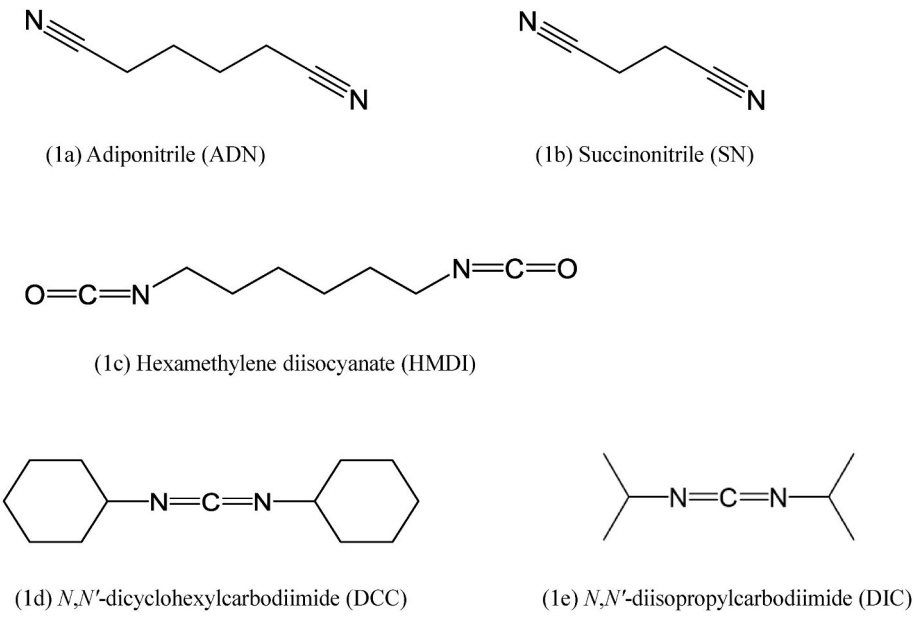

Fig. 1. Structures of the corrosion inhibition additives.

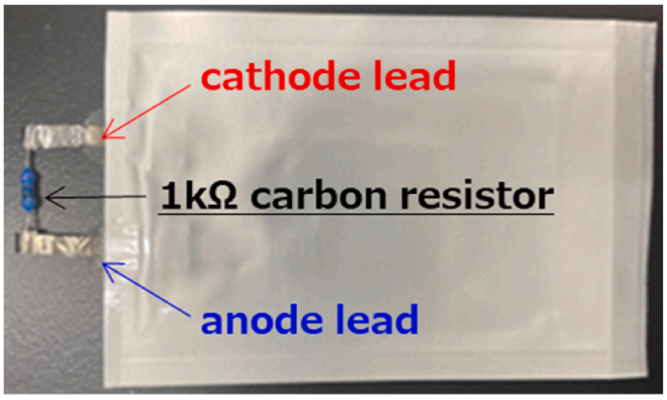

Fig. 2. Photo image of over-discharge test using laminated cell with a 1 kΩ carbon resistor connected to the cathode and anode leads.

electrolyte from the dissolution of the Cu current collector and precipitate on the anode during charging. This causes blackening of the Cu surface and an increase in the cell resistance, thus there is a concern that if it continues further, it may lead to a short circuit. Therefore, we designed an additive to prevent short circuits during over-discharge, aiming to suppress Cu dissolution and improve the battery performance.

In prior literature regarding suppressing the dissolution of the Cu current collector during over-discharge, Kim et al. published the mechanism of action of SN. According to this paper, it is known that SN not only prevents Al corrosion, but also has a corrosion-inhibiting effect on Cu. As a result, dissolution of the Cu current collector is suppressed by a passive layer of $Cu(SN)_2PF_6$ complexes on the Cu surface [7].

In this work, we focused on compounds with cumulated double bonds as additives to prevent short circuits during over-discharge, such as hexamethylene diisocyanate (HMDI, Fig. 1c) with the -N=C=O functional group, and *N*,*N*′-dicyclohexylcarbodiimide (DCC, Fig. 1d) and *N*,*N*′-diisopropylcarbodiimide (DIC, Fig. 1e) with the -N=C=N-functional group, and compared them to SN, which has the -C≡N functional group, such as that reported by Kim et al. In addition, SN was compared to ADN.

2. Experimental

2.1. Chemicals

Adiponitrile (ADN), hexamethylene diisocyanate (HMDI), *N*,*N*′-dicyclohexylcarbodiimide (DCC), and *N*,*N*′-diisopropylcarbodiimide (DIC) were purchased from Tokyo Chemical Industry Co., Ltd., and used without any further purification.

2.2. Battery performance evaluations

The experimental method using a laminated cell with a capacity of 14.8 mAh was based on our previously reported work [4]. It was utilized to evaluate the battery performances. The cathode active material in the cells was $LiCoO_2$ (Nichia Corporation), while the anode active material in the cells was artificial graphite (Resonac Corporation). The separator in the cells was a polyethylene separator with 20 μm thickness (Asahi Kasei Corporation). The electrolyte used in the cells was 1 M $LiPF_6$ [ethylene carbonate (EC)/ethyl methyl carbonate (EMC)/dimethyl carbonate (DMC) = 3/3/4 (vol%)] with 1 wt% vinylene carbonate (VC) (MU Ionic Solutions Corporation). The additives were ADN, HMDI, DCC, and DIC, and each added at 0.2 M to the electrolyte.

The charge/discharge test system for the battery performances was a TOSCAT-3100 (Toyo System Co., Ltd.) The charge/discharge evaluation was carried out at 25 °C. The cells were cycled at the rate of 0.1 C between 3.0-4.1 V for the first cycle and 3.0-4.2 V for the second cycle. The cycling evaluation was performed at the rate of 0.2 C between 3.0-4.2 V. The over-discharge test was performed by discharging to 3.0 V at 0.1 C, then storing the battery at 60 °C for 2 weeks with a 1 kΩ carbon resistor connected to the cathode and anode leads to a voltage of approximately 0 V as shown in Fig. 2.

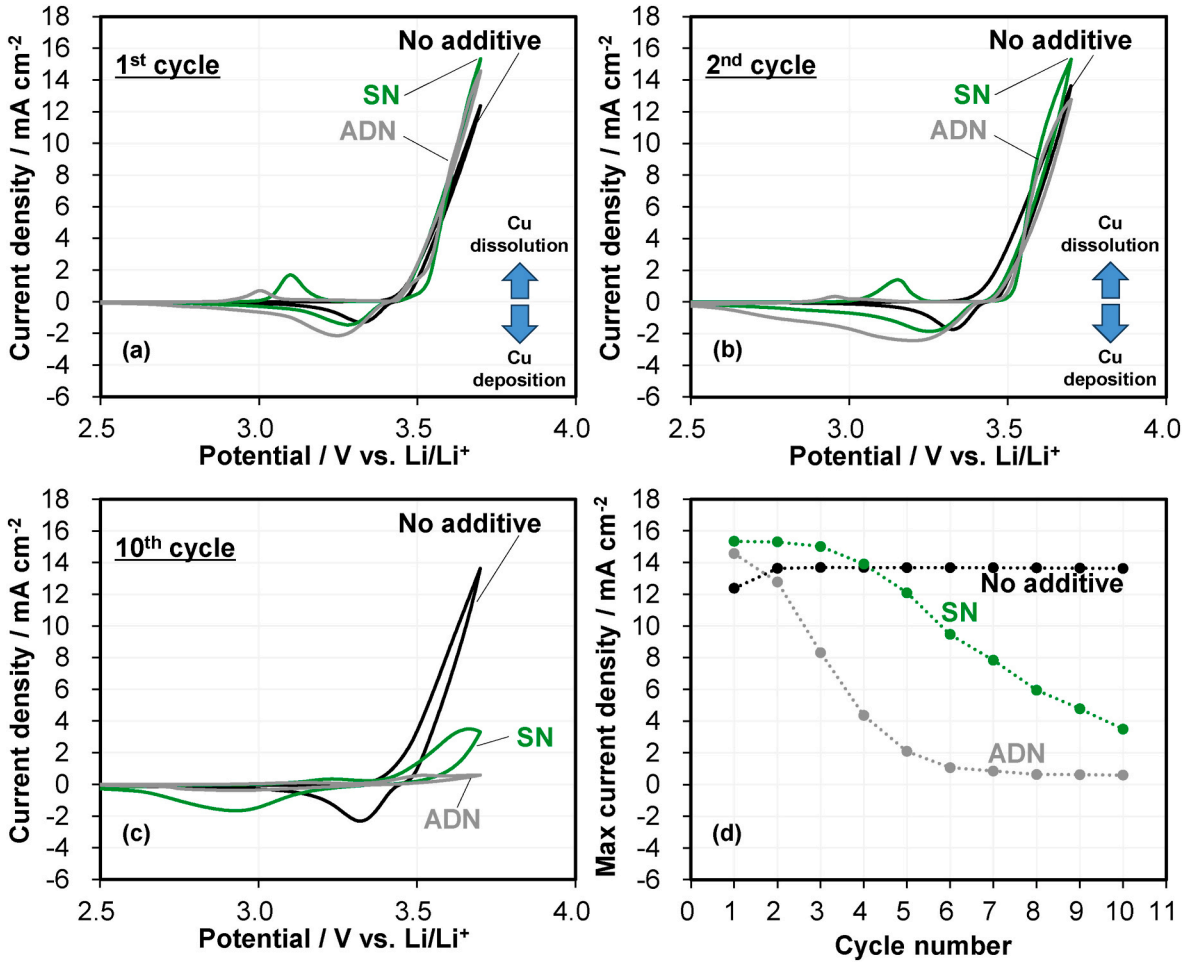

Fig. 3. CVs for (a) 1st cycle, (b) 2nd cycle, (c) 10th cycle and (d) maximum oxidation current in three-electrode glass cells (Cu/Li/Li) with SN and ADN Cu corrosion inhibition additives.

2.3. Cyclic voltammetry

Cyclic voltammetry (CV) tests were carried out in a Cu/Li/Li (w/c/r) three-electrode glass cell at 25 °C in the potential range of 2.5 and 3.7 V at the scanning rate of 5 mV s^{-1} using a SP-150 potentiostat (Biologic Science Instruments). The Cu working electrode was a 0.3 mm thick copper plate and the electrolyte was 1.2 M LiFSI EC/EMC/DMC = 3/3/4 (vol%). To reduce the potential fluctuation due to Cu metal deposition on the Li, a reference electrode was placed inside a polypropylene tube with a small polyolefin separator window.

2.4. Cu current collector analysis

The surface observation of the anode Cu current collector was carried out using scanning electron microscopy (SEM) and X-ray photoelectron spectroscopy (XPS). After the over-discharge test, the sample for analysis was prepared by cutting open a laminated cell and removing the anode electrode. It was washed three times using DMC to remove any electrolyte residue before the SEM and XPS analyses. The SEM was conducted using a JSM-7001F (JEOL). The XPS data were acquired by the 5600 ESCA system (ULVAC-PHI).

2.5. Synthesis of Cu^{2+} complexes for XPS measurements

The copper(II) hexafluorophosphate EMC complex $[Cu(EMC)_4](PF_6)_2$ was purchased from Kanto Denka Kogyo Co., Ltd.

In 500 cm^3 of DMC, 0.458 g (0.60 mmol) of blue-white $[Cu(EMC)_4](PF_6)_2$ was dissolved, then 0.648 g (6 mmol) of excess ADN was added. Since the target product $[Cu(ADN)_2](PF_6)_2$ was difficult to dissolve in DMC, a white pale precipitate was immediately formed. After waiting for complete precipitation, it was then filtered, washed with DMC and dried under reduced pressure.

As for the other target substances, 0.333 g (0.43 mmol) of blue-white $[Cu(EMC)_4](PF_6)_2$ was added to 6 cm^3 of DMC to make a suspension. When 0.151 g (0.73 mmol) of the DCC, 1.5 equivalents to the raw material, was added to the suspension, the solid in the suspension was reduced to about half. When another 1.5 equivalents of the DCC (0.155 g, 0.75 mmol) were added, the suspension was then almost completely dissolved and the solution turned dark green. Since the $[Cu(DCC)_3](PF_6)_2$ complex dissolves well in DMC, it was concentrated to dryness under reduced pressure to obtain $[Cu(DCC)_3](PF_6)_2$ as a green solid. In both cases, the synthesis was performed in a glove box with an Ar atmosphere, and subsequent steps were performed in flowing Ar gas. As a result of the XPS analysis (Fig. 7d), the atomic molar ratio (atomic %) of

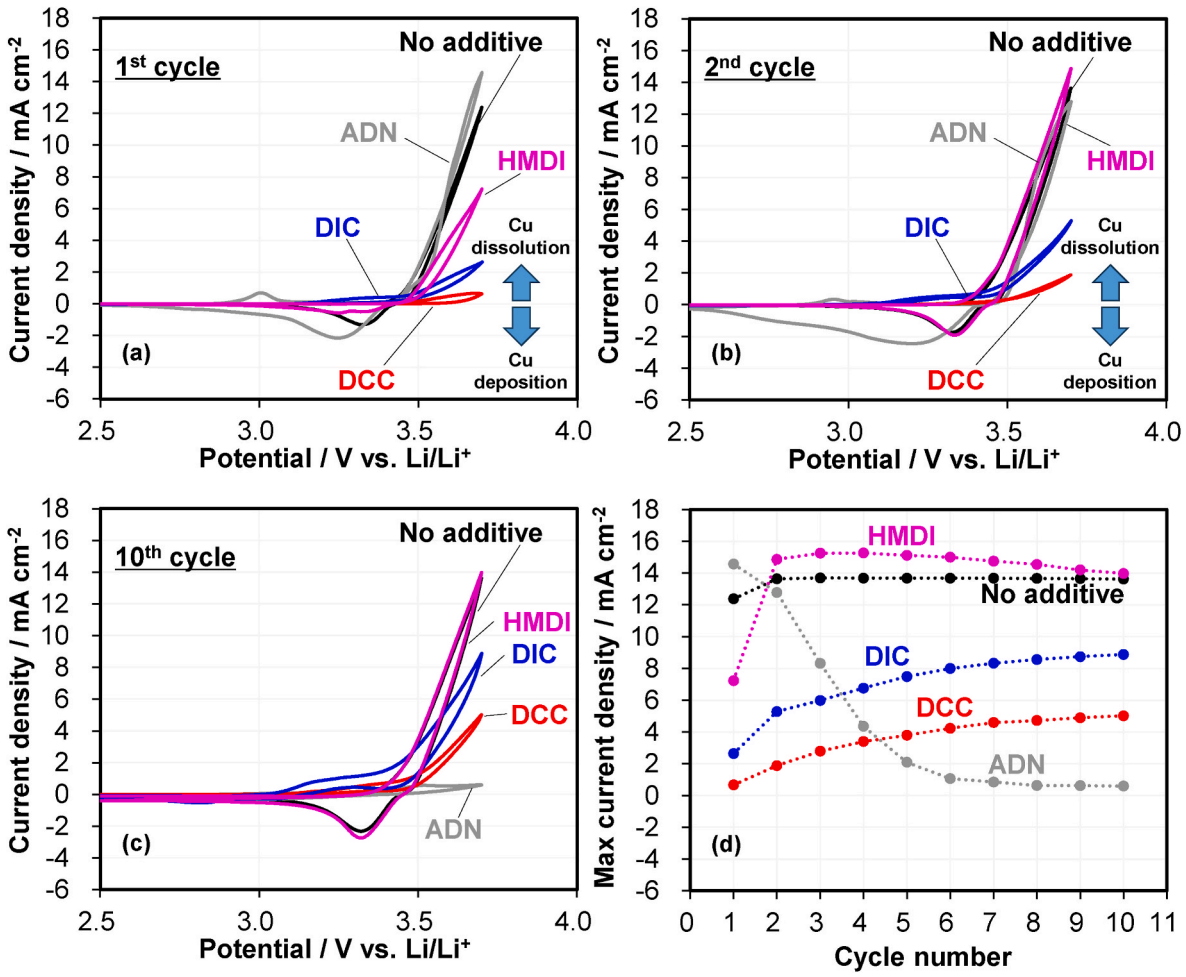

Fig. 4. CVs for (a) 1st cycle, (b) 2nd cycle, (c) 10th cycle and (d) maximum oxidation current in three-electrode glass cells (Cu/Li/Li) with Cu corrosion inhibition additives.

the DCC complex was C:63.8, N:7.5, O:4.2, F:19.4, P:2.8, and Cu:2.3. Based on this result, it was estimated that the DCC complex was [Cu(DCC)$_3$EMC](PF$_6$)$_2$.

3. Results and discussion

First, for SN and ADN, which are expected to prevent short-circuits during over-discharge, the Cu dissolution and deposition behaviors were investigated by cyclic voltammetry (CV) using a three-electrode glass cell. Fig. 3a shows the CV of the first cycle, Fig. 3b shows the CV of the second cycle, and Fig. 3c shows the CV of the tenth cycle. The area above 0 mA in the graph represents Cu dissolution and the area below 0 mA represents Cu deposition. Fig. 3d shows that with no additives, the dissolution/deposition behavior did not change from the first to the tenth cycle. On the other hand, with SN and ADN, the initial dissolution/deposition current was high, but both current values were gradually suppressed by the tenth cycle, indicating that ADN was more effective in suppressing the current than SN. Therefore, in this work, we used ADN due to its superior performance in suppressing Cu dissolution compared to SN.

Next, for ADN, HMDI, DCC, and DIC, the dissolution and deposition behavior of Cu was investigated by CV using a three-electrode glass cell. Fig. 4a shows the CV of the first cycle, Fig. 4b shows the CV of the second cycle, and Fig. 4c shows the CV of the tenth cycle. The dissolution/deposition behavior of HMDI was similar to that of no additive from the second to the tenth cycle. With DCC and DIC in Fig. 4d, the initial dissolution/deposition currents were negligibly low and the Cu deposition current was characteristically suppressed from the first cycle. Although Cu dissolution gradually increases with cycles, it has almost reached saturation. The dissolution current at the tenth cycle is smaller than that without additive, especially for DCC than for DIC. These results suggested that dinitrile compounds, such as SN and ADN, and cumulative double bond compounds, such as DCC and DIC, are expected to have very different mechanisms of action.

Fig. 5a shows the charge-discharge curves for the second cycle for the electrolyte with ADN, HMDI, DCC, and DIC. The results indicated that only HMDI showed an increase in polarization and a decrease in capacity. The cycle performance shown in Fig. 5b also showed that HMDI exhibited a significant cycling degradation from the beginning of the cycle. The reason for this may be that HMDI is easily reductively decomposed, so some of it is decomposed at the anode. In addition, HMDI easily reacts with HF and moisture, thus there is concern that it

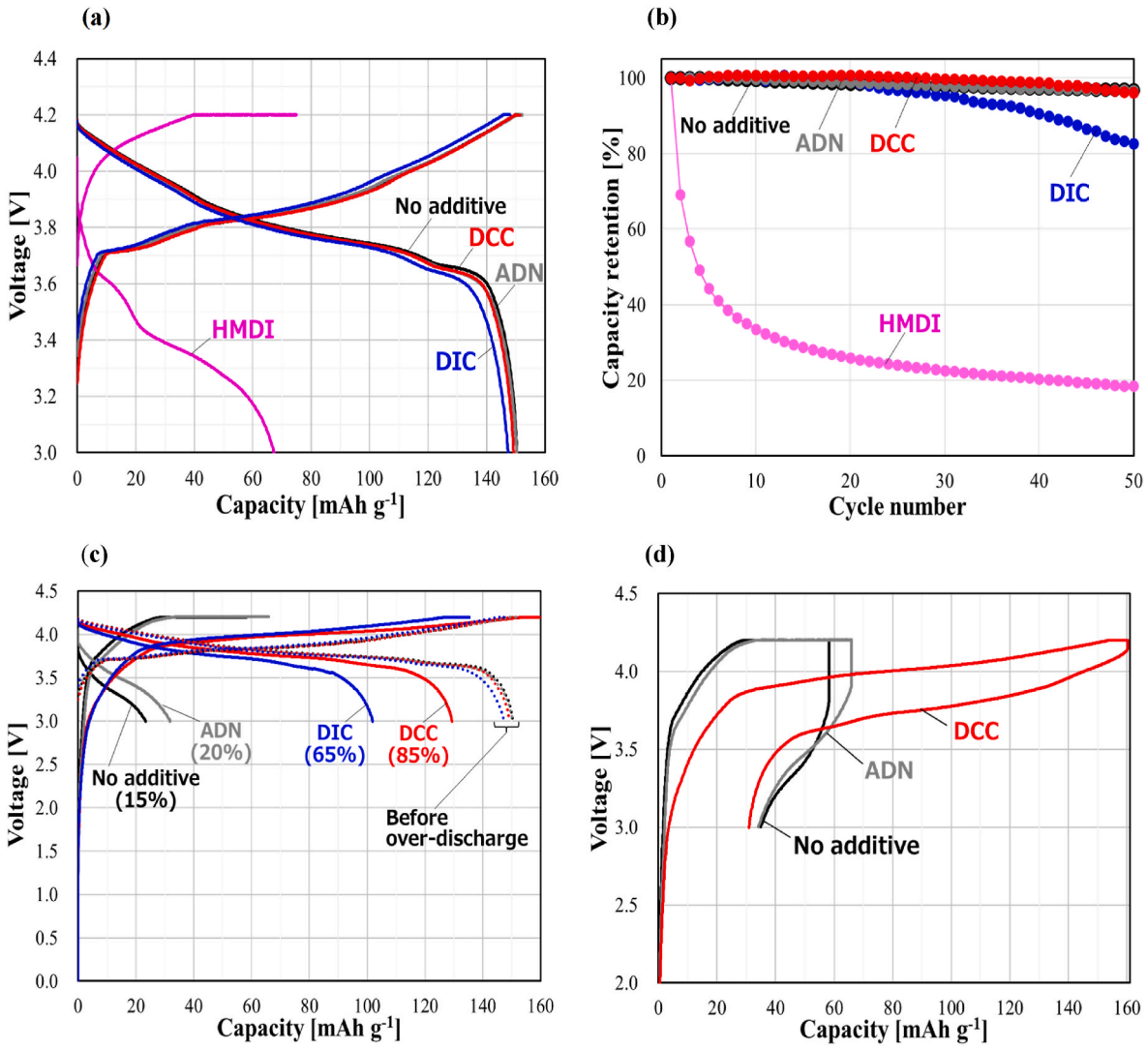

Fig. 5. (a) 2nd cycle charge-discharge curves and (b) cycle performances of the cells with -C≡N, -N=C=O, and -N=C=N- bond compounds, and (c) charge-discharge curves and capacity recovery rates of the cells with -C≡N and -N=C=N- bond compounds and (d) charge-discharge curves of ADN and DCC after over-discharge test.

may easily decompose. DIC also showed a slight degradation trend compared to ADN and DCC. The reason for this may be that DIC with isopropyl groups is less electron-donating than DCC with cyclohexyl groups, and thus has less ability to suppress Cu dissolution as the coordination strength decreases. Fig. 5c showed the charge/discharge behavior and the capacity recovery rate after the over-discharge test. Without the additive, the polarization was very high, and with ADN, the polarization was also high and the recovery rate was only 20 %. The recovery rates (15 % and 20 %) indicated that the effect was limited. On the other hand, the capacity recovery rates of DCC and DIC were 85 % and 65 %, respectively, and found to be good.

In fact, when we observed the surface of the Cu current collector after the over-discharge test in Fig. 6 (from a to h), in the case of no additive, there were many visible black spots and pitting corrosion on the back side of the anode electrode. Based on this observation, it was found that there was dissolution of the Cu current collector. However, the number of black spots and pitting corrosion were significantly reduced in the electrolyte containing each additive, indicating that it is effective in preventing the dissolution of the Cu current collectors. Among them, it was found that while ADN changed color due to something covering the surface, the SEM results revealed that only ADN had precipitates on its surface. On the other hand, DCC and DIC retained their Cu luster and no precipitates were observed.

According to the enlarged SEM in Fig. 6 (from i to l), ADN had precipitates on the Cu surface, and the cross-sectional SEM showed that the precipitates were found everywhere (red arrow part), including inside the Cu foil and between the anode active materials. This suggested that ADN loses its Cu luster due to the presence of the precipitates, and these precipitates increased the polarization and reduced the recovery rate after over-discharge.

In each XPS depth profile of Fig. 7 (from a to c), the left side shows the surface element ratio, and the right side shows the internal element

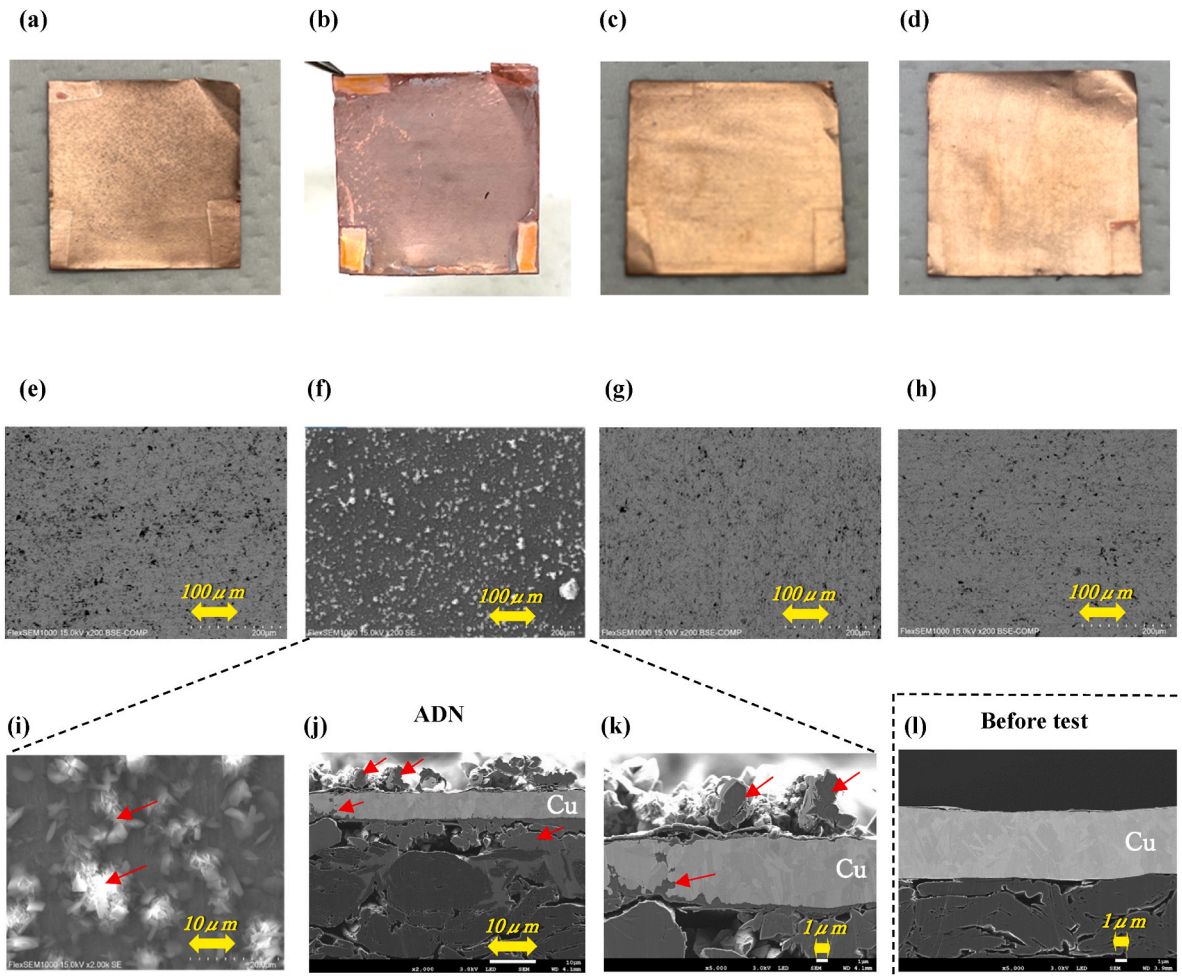

Fig. 6. Photo images (from a to d) and corresponding SEM images (×200) (from e to h) of Cu substrates (back side of anode) after over-discharge test at about 0 V for 2 weeks at 60 °C: (a, e) No additive, (b, f) 0.2 M ADN, (c, g) 0.2 M DCC, and (d, h) 0.2 M DIC, and SEM images of Cu substrates (back side of anode) of the cell with 0.2 M ADN after over-discharge test (from i to k) or before test (l): (i) surface SEM (×2,000), (j) cross-sectional SEM (×2,000), (k) cross-sectional SEM (×5,000), and (l) cross-sectional SEM (×5,000) before test.

ratio. Compared to no additive, the ADN Cu current collector, in which this precipitate is generated, has a higher abundance ratio of C and N from the surface to the inside, and a lower abundance ratio of Cu, suggesting that ADN is forming a thick film. On the other hand, since the ratio of the C element on the outermost surface of DCC is slightly higher, it is inferred that something slightly exists on the outermost surface. This clearly supports the fact that the Cu surface states of ADN and DCC are different.

An XPS analysis of the N1s spectra of the Cu substrate of the anodes after over-discharge shown in Fig. 8 (from a to c) indicates that, compared to no additive, ADN forms a film containing N from the surface to the inside, as previously reported. On the other hand, DCC suggests an increase in a layer containing N on the outermost surface. Based on this result, we considered that DCC does not form precipitates like ADN, and a thin N-containing layer is formed on the outermost surface, thus the capacity recovery rate after the over-discharge test is not worse.

To further clarify the XPS analysis, the same XPS analyses were performed on copper complex compounds of $[Cu(ADN)_2](PF_6)_2$ and $[Cu(DCC)_3EMC](PF_6)_2$ synthesized from $[Cu(EMC)_4](PF_6)_2$ using the process described in Experimental § 2.5. From the XPS analysis of the N1s spectra of the Cu complex compounds in Fig. 8 (from d to f), the peak position of each film on the Cu substrate was almost the same as that of each complex compound. In addition, the peak positions of the complex compounds are different between $[Cu(ADN)_2](PF_6)_2$ (Fig. 8e) and $[Cu(DCC)_3EMC](PF_6)_2$ (Fig. 8f), and the peak appearing at 400 eV for $[Cu(ADN)_2](PF_6)_2$ was attributed to the -C≡N bond, while the peak appearing at 401 eV for $[Cu(DCC)_3EMC](PF_6)_2$ was attributed to the -N=C=N- bond.

Regarding the XPS analysis of the Cu2p spectra of the Cu substrate of the anodes after the over-discharge test in Fig. 8 (from g to i), a peak assigned to $Cu(CN)_x$ appears in ADN, suggesting a complex formation. On the other hand, in DCC, only the zero-valent Cu peak derived from the Cu substrate seemed to be observed. However, from the XPS analysis of the Cu2p spectra of the Cu complex compounds in Fig. 8 (from j to l), it was determined that $[Cu(ADN)_2](PF_6)_2$ and $[Cu(DCC)_3EMC](PF_6)_2$ had both the monovalent Cu peak appearing at 933 eV and the divalent

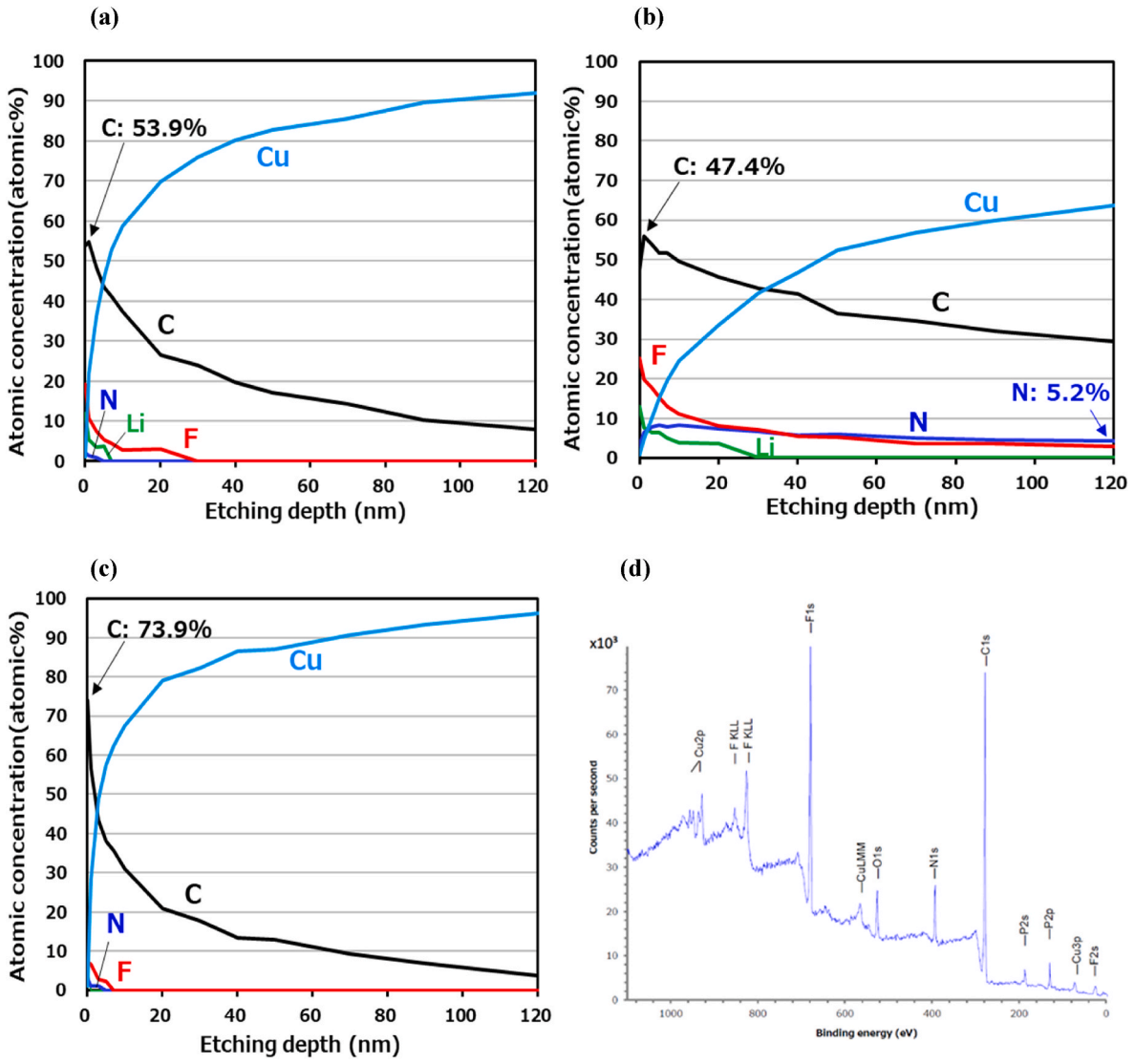

Fig. 7. XPS depth profiles of Cu substrate of the anodes after over-discharge test for the cells with: (a) No additive, (b) 0.2 M ADN, (c) 0.2 M DCC, and (d) XPS analysis of wide-scan spectra of the DCC complex on the surface.

Cu peak (like $[Cu(EMC)_4](PF_6)_2$, Fig. 8j) appearing at 934–947 eV. Based on the results of the chemical bond state analysis, the existence ratios of Cu(I): Cu(II) were $[Cu(ADN)_2](PF_6)_2 = 31 : 69$ (Fig. 8k) and $[Cu(DCC)_3EMC](PF_6)_2 = 75 : 25$ (Fig. 8l). It was found that the valence of Cu in $[Cu(ADN)_2](PF_6)_2$ was mainly divalent, whereas the valence of Cu in $[Cu(DCC)_3EMC](PF_6)_2$ was mainly monovalent. Therefore, it was suggested that ADN and DCC form monovalent and divalent mixed Cu complexes that also contain PF_6 ions when Cu ions were dissolved in the electrolyte during over-discharge. Also, since the DCC complex is mainly monovalent, it is postulated that it overlapped with the peak of the zero-valent Cu substrate in Fig. 8i.

The separately synthesized $[Cu(ADN)_2](PF_6)_2$ had an extremely low solubility and white precipitation quickly occurred, so the precipitates in Fig. 6 (f, i, j, k) are considered to be white $[Cu(ADN)_2](PF_6)_2$. Similarly, $[Cu(DCC)_3EMC](PF_6)_2$ had an extremely high solubility, did not easily precipitate, and was a green solution, suggesting that the surface in Fig. 6g was covered with a layer of green $[Cu(DCC)_3EMC](PF_6)_2$. In a work by Kim et al., SN forms a complex with the dissolved Cu forming a passive layer on the Cu surface and inhibiting subsequent Cu dissolution. In contrast, our DCC with the -N=C=N- functional group is characterized by the fact that the DCC complex of Cu does not deposit. Presumably, DCC forms a complex on the Cu surface to form a barrier layer from the moment it is added to the electrolyte. The important point of this research is that we found that the Cu complex in DCC does not deposit even if there is some Cu dissolution.

The degradation factor of recovery capacity after over-discharge depends not only on Cu corrosion but also on its suppression mechanism. As shown in Fig. 6 (f, i, j, k), the ADN complex of Cu can precipitate on the Cu foil surface and stop further Cu deposition. However, the ADN complex of Cu also deposits on the graphite anode surface,

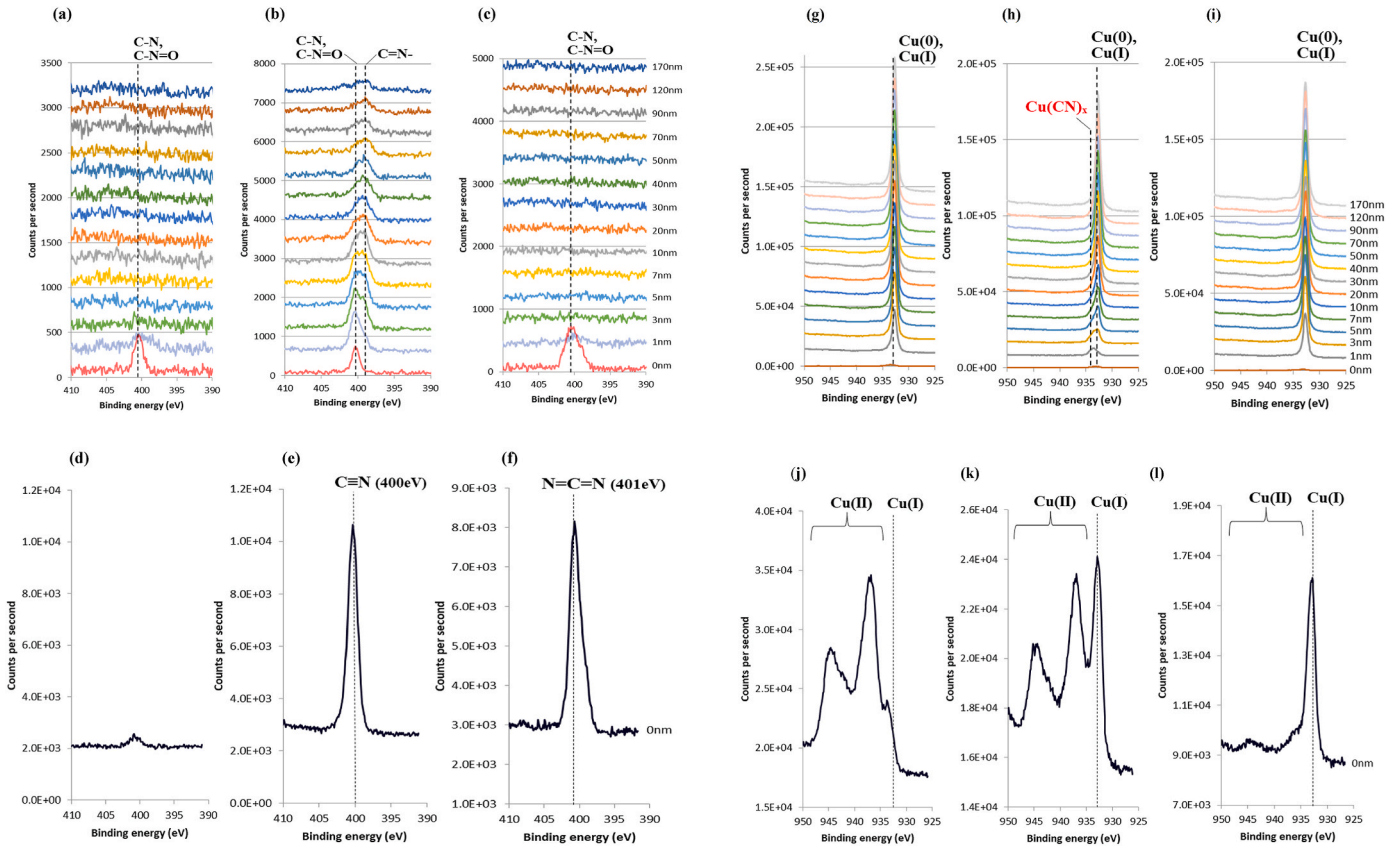

Fig. 8. XPS analysis of N1s (from a to c) or Cu2p (from g to i) spectra of Cu substrate of the anodes after over-discharge test for the cells with: (a, g) No additive, (b, h) ADN, and (c, i) DCC, and N1s (from d to f) or Cu2p (from j to l) spectra of Cu complex compounds on the surface: (d, j) $[Cu(EMC)_4](PF_6)_2$, (e, k) $[Cu(ADN)_2](PF_6)_2$, and (f, l) $[Cu(DCC)_3EMC](PF_6)_2$.

Table 1
Summary of cell performances using electrolytes with Cu corrosion inhibition additives.

Additives	No additive	ADN	DCC	DIC
• Capacity at 2nd cycle (4.2–3.0 V)	149 mAh g^{-1}	149 mAh g^{-1}	149 mAh g^{-1}	147 mAh g-1
Cycling performance (50 cyc at 25 °C)	96 %	96 %	96 %	83 %
Cu corrosion behavior after over-discharge (Visual and SEM)	Blackspots and pitting corrosion increase	Blackspots and pitting corrosion significantly decrease		
Precipitates	–	Existing	None	
Solubility of Cu complex with additives	–	Extremely low	Extremely high	–
Surface film or layer on Cu after over-discharge	None	Thick film (μm order) containing C and N elements	Thin layer (nm order) containing C and N elements	–
Capacity recovery after over-discharge	15 %	20 %	85 %	65 %

resulting in increased polarization as shown in Fig. 5d and a lower recovery capacity after over-discharge. On the other hand, as shown in Fig. 6g, the DCC complex of Cu does not deposit on the surface of Cu foil or graphite anode, but forms a thin film (thin layer) of nm order as a barrier layer as shown in Fig. 7c and Fig. 8c. Therefore, the polarization after over-discharge is quite small, and we believe that there is little effect on the recovery capacity after over-discharge.

Table 1 shows a summary of the cell performances using electrolytes with the Cu corrosion inhibition additives. As shown in Table 1, it can be concluded that DCC is a promising additive that can suppress Cu dissolution during over-discharge and has excellent battery performances.

4. Conclusion

This work investigated additives that can both suppress the dissolution of the Cu current collector and improve the battery performance during over-discharge. ADN, DCC, and DIC were all found to have good second cycle discharge capacities and cycling performances, but HMDI was found to undergo a cycling degradation. For ADN, DCC, and DIC, which have good cycling performances, we examined the black spots after over-discharge and found that they all showed a decrease, indicating that they were effective in preventing Cu leaching. The analysis revealed that ADN forms a thick film on the order of μm, while DCC forms a thin layer on the order of nm. This suggests that the DCC

complex with the cumulated double bonds does not form a white precipitate like the ADN complex. The recovery rates after over-discharge were high for DCC and DIC, and DCC, in particular, showed a good performance for both the second cycle discharge capacity and cycle performances. These results indicated that additives with the carbodiimide groups (-N=C=N-) are useful as new types of short circuit prevention additives during over-discharge that can both prevent Cu leaching and reduced battery performance.

CRediT authorship contribution statement

Masaki Deguchi: Writing – review & editing, Writing – original draft, Investigation, Data curation. **Yanko Marinov Todorov:** Supervision, Data curation, Conceptualization. **Koji Abe:** Writing – review & editing, Supervision, Data curation, Conceptualization.

Declaration of competing interest

The authors declare that they have no known competing financial interests or personal relationships that could have appeared to influence the work reported in this paper.

Appendix A. Supplementary data

Supplementary data to this article can be found online at https://doi.org/10.1016/j.jpowsour.2024.235613.

Data availability

The authors do not have permission to share data.

References

[1] K. Abe, Y. Ushigoe, K. Kawabe, Advanced Automotive Battery Conference on Large Lithium Ion Battery Technology and Application (LLIBTA) Symposium, Pasadena, USA, Jan, 2011, pp. 24–28.
[2] K. Abe, T. Hattori, Y. Matsumori, Non-aqueous electrolytic solution and lithium battery, US patent 9 (742) (2017) 33 (UBE Co., Ltd.) applied in 2002.
[3] K. Abe, T. Hattori, Y. Matsumori, Non-aqueous electrolytic solution and lithium battery, US patent 9 (742) (2018) 33 (UBE Co., Ltd.) applied in 2002.
[4] M. Deguchi, Y.M. Todorov, K. Abe, Electrochim. Acta 469 (2023) 143267, https://doi.org/10.1016/j.electacta.2023.143267.
[5] K. Matsumoto, K. Inoue, K. Nakahara, R. Yuge, T. Noguchi, K. Utsugi, J. Power Sources 231 (2013) 234, https://doi.org/10.1016/j.jpowsour.2012.12.028.
[6] K. Park, S. Yu, C. Lee, H. Lee, J. Power Sources 296 (2015) 197, https://doi.org/10.1016/j.jpowsour.2015.07.052.
[7] Y.-S. Kim, S.-H. Lee, M.-Y. Son, Y.-M. Jung, H.-K. Song, H. Lee, ACS Appl. Mater. Interfaces 6 (2014) 2039–2043, https://doi.org/10.1021/am405092y.